THE JOURNAL OF BIOLOGICAL CHEMISTRY VOL. 285, NO. 25, pp. 19277–19287, June 18, 2010
© 2010 by The American Society for Biochemistry and Molecular Biology, Inc. Printed in the U.S.A.

Amelogenin-Collagen Interactions Regulate Calcium Phosphate Mineralization *in Vitro*[*] [S]

Received for publication, October 27, 2009, and in revised form, March 17, 2010 Published, JBC Papers in Press, April 19, 2010, DOI 10.1074/jbc.M109.079939

Atul S. Deshpande[‡], Ping-An Fang[‡], James P. Simmer[§], Henry C. Margolis[¶], and Elia Beniash[‡1]

From the [‡]Department of Oral Biology, Center for Craniofacial Regeneration, University of Pittsburgh School of Dental Medicine, Pittsburgh, Pennsylvania 15261, the [§]Department of Biologic and Materials Science, University of Michigan School of Dentistry, Ann Arbor, Michigan 48109, and the [¶]Department of Biomineralization, The Forsyth Institute, Boston, Massachusetts 02115

Collagen and amelogenin are two major extracellular organic matrix proteins of dentin and enamel, the mineralized tissues comprising a tooth crown. They both are present at the dentin-enamel boundary (DEB), a remarkably robust interface holding dentin and enamel together. It is believed that interactions of dentin and enamel protein assemblies regulate growth and structural organization of mineral crystals at the DEB, leading to a continuum at the molecular level between dentin and enamel organic and mineral phases. To gain insight into the mechanisms of the DEB formation and structural basis of its mechanical resiliency we have studied the interactions between collagen fibrils, amelogenin assemblies, and forming mineral *in vitro*, using electron microscopy. Our data indicate that collagen fibrils guide assembly of amelogenin into elongated chain or filament-like structures oriented along the long axes of the fibrils. We also show that the interactions between collagen fibrils and amelogenin-calcium phosphate mineral complexes lead to oriented deposition of elongated amorphous mineral particles along the fibril axes, triggering mineralization of the bulk of collagen fibril. The resulting structure was similar to the mineralized collagen fibrils found at the DEB, with arrays of smaller well organized crystals inside the collagen fibrils and bundles of larger crystals on the outside of the fibrils. These data suggest that interactions between collagen and amelogenin might play an important role in the formation of the DEB providing structural continuity between dentin and enamel.

Dentin and enamel, the two mineralized tissues that comprise a tooth crown, are strikingly different in terms of their compositional, structural, and mechanical properties (1). Despite these differences, dentin and enamel work together for decades under severe mechanical stress, without delamination or catastrophic failure.

Dentin is a mineralized tissue similar to bone, comprised primarily of fibrillar collagen type I, carbonated apatite and water (2). There are other so-called noncollagenous macromolecules present that, in total, represent less then 10% by mass of organic material, although they play important roles in the formation and function of these tissues. All bone materials share the same basic building block, a collagen fibril, in which plate-shaped apatitic crystals are organized in parallel arrays with their c-axes co-aligned with the long axis of the fibril (2–4). Collagen type I triple helical molecules, are super-coiled assemblies of two identical α1-chains and one α2-chain with a different sequence (5, 6). Each chain contains more than 1000 amino acids and is primarily composed of Gly-X-Y repeats, where amino acids proline (Pro) and hydroxyproline (Hyp) predominantly occupy X and Y positions. All three chains in the molecule adopt a polyproline II (PPII)-like structure, which is stabilized by direct and water mediated inter- and intra-chain hydrogen bonds (5, 6). Collagen fibrils form via a self-assembly process in which collagen triple helices aggregate with their long axes in parallel. Within the fibril there is a linear shift of some 67 nm (D-period) between neighboring molecules generating a periodic structure along the long axis of the fibril. This staggered fibril assembly leaves gaps of 0.6D between the ends of co-linear collagen molecules and an 0.4D overlap region for every 67-nm fibril repeat (7, 8). It has been demonstrated in a number of reports that collagen fibrils alone do not affect the formation, morphology, and organization of calcium phosphate crystals (9–11), whereas the noncollagenous proteins have been shown to regulate collagen mineralization in bones and dentin (12–14). Furthermore, the noncollagenous proteins often bind to specific motifs on collagen molecules, and such interactions are believed to play important roles in the regulation of collagen mineralization (15–18).

Mature enamel is the hardest tissue in the body, comprised of ~95% apatitic mineral, 4% water and less than 1% of organic matrix. In contrast, in forming enamel the organic matrix comprises roughly 20% while mineral and water account for 30 and 50% respectively. The basic building block of enamel is an enamel rod, a dense array of needle-shaped carbonated apatite crystals, roughly 50 nm across and tens of microns long, with their c-axes co-aligned (1). These mineral rods form an intricate three-dimensional interwoven microstructure, which contributes to the high fracture resistance of enamel. A number of proteins were identified in the transient enamel matrix, with amelogenin constituting more than 90% of the enamel matrix. Amelogenin is a fairly hydrophobic protein comprised of N-terminal tyrosine-rich domain (TRAP), central proline-rich domain, and a C-terminal hydrophilic telopeptide (19). Amelogenin monomers adopt an extended conformation in solution with a large fraction of PPII type helix (20–24).

* This work was supported, in whole or in part, by National Institutes of Health NIDCR Grant DE016703 (to E. B.).

[S] The on-line version of this article (available at http://www.jbc.org) contains supplemental Figs. S1–S5.

[1] To whom correspondence should be addressed: University of Pittsburgh School of Dental Medicine, Dept. of Oral Biology, Center for Craniofacial Regeneration, 589 Salk Hall, 3501 Terrace St., Pittsburgh, PA 15261. Tel.: 412-6480108; Fax: 412-6246685; E-mail: ebeniash@pitt.edu.

This is an Open Access article under the CC BY license.

Amelogenin self-assembles at physiological conditions into nanospheres 10–20 nm in diameter, which aggregate into chain-like higher-order structures (25, 26). It has been shown in *in vitro* mineralization experiments that amelogenin regulates morphology and organization of mineral particles, leading to the formation of parallel arrays of elongated apatitic crystals, similar to the organization in enamel rods (27, 28).

Dentin and enamel are bound together at the dentin-enamel boundary (DEB),[2] a robust interface, which contributes to the remarkable mechanical resilience of a tooth (29–34). DEB is a part of a much broader transitional zone, called Dentino-Enamel Junction (DEJ). The DEJ is a several hundred micron thick layer with graded mechanical properties. Its main function is the transfer of mechanical forces from the hard and brittle enamel layer to tough and soft dentin (35, 36). Structurally, the DEB can be identified as consisting of the outer portion of mantle dentin and the most basal layer of enamel, the so-called aprismatic enamel (34). These two layers are distinctly different from the bulk of their corresponding tissues. Mantle dentin is a 10–20-μm thick layer adjacent to enamel. It contains bundles of mineralized collagen fibrils, oriented normal to the DEB plane, the so-called von Korff fibers, in contrast to the bulk of dentin tissue, in which collagen fibrils are oriented parallel to the DEB plane (15, 35, 37). Enamel adjacent to the mantle dentin lacks the typical prismatic architecture, and is comprised of mineral crystals also oriented normal to the DEB plane, as are the crystals in Von Korff collagen fibrils.

The DEB is the first structure formed during tooth development (1). Before the onset of mineralization, odontoblasts and ameloblasts form two juxtaposed cell layers. Odontoblasts start to deposit organic matrix of the mantle dentin, which begins to mineralize soon after its deposition. The beginning of dentin mineralization triggers the enamel deposition by ameloblasts which start to withdraw from the mineralized dentin layer leaving behind nascent enamel crystals of aprismatic enamel embedded in a protein gel. The fact that dentin mineralization precedes enamel formation and that initial enamel crystals form on top of the mineralized dentin and have similar crystallographic orientation as the crystals in von Korff fibrils led to the hypothesis that the mineralized mantle dentin serves as a template for enamel crystals (38, 39). Yet, other researchers have not found any evidence of epitaxial relationships between dentin and enamel mineral; instead it has been proposed that the dentin proteins or mineral crystals at the DEJ dictate the enamel matrix organization, which in turn influences crystal organization (40).

Besides their distinct structural organization, mantle dentin and aprismatic enamel have unique protein compositions, different from the typical protein composition of bulk dentin and enamel tissues. Specifically, a number of enamel proteins including amelogenin, the major protein of forming enamel, is also expressed by odontoblasts at the onset of dentin formation and found in the mantle dentin (41, 42), while the major non-collagenous dentin protein DSPP is transiently expressed by early ameloblasts (43, 44). Such unique extracellular matrix composition of mantle dentin and aprismatic enamel at the DEB is likely to be essential for the proper formation and function of this interface. This notion is supported by the studies of the hereditary tooth diseases in humans and experiments with animal models, which demonstrate that mutations in a number of extracellular tooth proteins lead to the weakening of the DEB and the breaking off of tooth enamel leading to exposure of the dentin surface (45–50). Hence, it is essential to understand how the individual proteins present at this boundary, as well as more complex systems including multiple ECM components, affect calcium phosphate mineralization.

In vitro mineralization experiments are widely used to understand the functional properties of proteins involved in mineralization (51, 52). These *in vitro* systems are powerful research tools and have numerous advantages, such as the ability to carry out experiments in a systematic manner and under controlled conditions. Such analytical approaches allow for the study of one or more individual elements of a mineralization system in isolation. At the same time, these *in vitro* systems, by their nature, are less complex than the *in vivo* environment, which involve multiple interactions which are extremely difficult to reproduce *in vitro*. Nevertheless, synthesis of the data obtained in *in vitro* experiments and *in vivo* observations can lead to better understanding of complex biomineralization systems such as that associated with the DEB.

To provide new insights into the supramolecular protein assemblies and forming mineral at initial stages of tooth formation at the DEB we set out to study interactions between collagen and amelogenin, two major matrix proteins in a developing tooth, and the effects of these interactions on calcium phosphate mineralization *in vitro*.

EXPERIMENTAL PROCEDURES

Preparation of Purified Collagen Solution—The collagen purification was carried out in accordance with well established published procedures (9, 53). Acidic solution of type I collagen was obtained from rat-tail tendon. The tendons were collected from 4–8-week-old rats and washed in protease inhibitor buffer. Then the tendons were briefly rinsed in deionized water, homogenized, and solubilized in 2 mM HCl (pH 2.8). The collagen solution was centrifuged at 25,000 × *g* to remove aggregates. Collagen was then purified by several cycles of selective salt precipitation followed by acid dissolution as reported elsewhere (9, 53). The quality and purity of the preparation was verified by SDS-PAGE gel electrophoresis (supplemental Fig. S1).

Stock Solutions—High purity $CaCl_2{\cdot}2H_2O$, $Na_2HPO_4{\cdot}7H_2O$, $NaH_2PO_4{\cdot}2H_2O$, KH_2PO_4, and NaOH were obtained from Sigma-Aldrich. A 10× PBS buffer with 10.58 mM KH_2PO_4, 29.66 mM $Na_2HPO_4{\cdot}7\ H_2O$, and 1551.72 mM NaCl was prepared in deionized distilled water (DDW) with the resistivity of 18.2 MΩ cm. The pH of this buffer solution was adjusted to 7.2 (pH 7.8 at 1× dilution) using NaOH. Stock solutions of $CaCl_2$ (6.68 mM) $Na_2HPO_4{\cdot}2\ H_2O$ (4 mM) and NaOH (5 mM) were prepared using DDW. Lyophilized recombinant protein rM179 was dissolved in filtered DDW to give a concentration 2 mg/ml.

[2] The abbreviations used are: DEB, dentin-enamel boundary; PBS, phosphate-buffered saline; BSA, bovine serum albumin; TEM, transmission electron microscopy; SAED, selected area electron diffraction; DDW, deionized distilled water.

the solution was maintained at 4 °C for 48 h to facilitate dissolution. rM179 was prepared and purified as previously described (54).

Assembly of Collagen Fibrils—To achieve effective removal of cross-linked collagen and to obtain collagen fibrils with larger diameters, additional steps were taken prior to the assembly of collagen fibrils on TEM grids. Typically, 9 ml of acidic collagen solution and 1 ml of 10× PBS solution were mixed together to obtain 0.1–0.2% collagen solution in 1× PBS. This solution was incubated in a closed vial at 37 °C for 3 h. The incubation resulted in a gel of self-assembled collagen fibrils. The resultant gel was stored at 4 °C for typically 1 week upon which the gel resolves into a clear solution. This solution was centrifuged at 25,000 × *g* at 4 °C for 30 min. The supernatant was collected and stored at 4 °C. To obtain a thin layer of collagen fibrils, a 20-μl droplet of this mixed solution was placed on an inert polyethylene substrate in a humidity chamber, and a carbon coated Ni grid (EMS, Hatfield, PA) was placed on top of the droplet. The humidity chamber was sealed and the sample was incubated at 37 °C for 3 h. After the incubation, the grid was quickly washed with DDW and blotted against a filter paper and air-dried.

Amelogenin Assembly in the Presence of Collagen Fibrils—Recombinant full-length mouse amelogenin rM179 was produced and purified according to an established protocol (54). The stock solutions of rM179 and NaOH were mixed together to obtain solution of 0.5 mg/ml amelogenin in 1.25 mM NaOH. A 20-μl droplet of this solution was placed on an inert polyethylene substrate in a humidity chamber. A TEM grid-coated with thin layer of collagen fibrils as obtained above was placed on top of this droplet. The samples were incubated at 37 °C for 4–16 h. After the incubation, the grid were quickly washed with DDW, blotted against a filter paper and air-dried. For TEM analysis, the grids were negatively stained with 1% uranyl acetate.

Immunogold Labeling of Amelogenin Assembled in the Presence of Collagen Fibrils—Immunogold labeling was carried out on samples with amelogenin assembled in the presence of collagen fibrils to localize amelogenin with respect to collagen fibrils and to rule out possibility of physical adsorption or drying artifacts in negatively stained samples. The TEM grids as prepared above were incubated for 1 h with a solution containing rabbit anti-mouse amelogenin antibodies. The original antiserum was diluted 30× in PBS containing 0.5% BSA. The grids were then washed for 3 min with 0.5% BSA in PBS, and the washes were repeated four times. They were then incubated with donkey anti-rabbit antibodies conjugated with 5-nm gold particles after the original solution was diluted 25 × with 0.5% BSA in PBS. The grids were washed five times, as described above. Finally the grids were washed with DDW, blotted against a filter paper, and air-dried.

Mineralization in the Presence of Amelogenin and Pre-assembled Collagen Fibrils—To 5 μl of 4 mM $Na_2HPO_4 \cdot 2H_2O$ solution, 5 μl each of 5 mM NaOH, 2 mg/ml amelogenin, and 6.68 mM $CaCl_2 \cdot 2H_2O$ were, respectively, to achieve final concentrations of 1.25 mM NaOH, 1.67 mM C $CaCl_2$, 1 mM Na_2HPO_4, and 0.5 mg/ml amelogenin. pH of the mineralization solution was adjusted to pH 8.2. A 20-μl droplet of this solution was place in humidity chamber and a TEM grid-coated with thin layer of collagen fibrils as obtained above was placed on top of this droplet. The samples were incubated at 37 °C for 2, 3, 4, and 16 h. After incubation, the grid were quickly washed with DDW, blotted against a filter paper, and air-dried. pH measurements of the mineralization solutions were taken before and after the experiments, using a MI-414 6 cm combination microelectrode (Microelectrodes, Bedford, NH).

TEM and Selected Area Electron Diffraction (SAED) Analysis—A JEOL 1210 TEM microscope operated at 100 kV and JEOL 2000EX operated at 200 kV were used to study TEM and SAED of all samples. The micrographs were recorded using an AMT CCD camera (AMT, Danvers, MA). An aluminum film coated TEM grid (EMS Hatfield, PA) were used as a standard to calibrate SAED patterns for *d*-spacing calculations. The micrographs were analyzed using ImageJ 1.38× image processing software (Bethesda, MD). For statistical analyses of dimensions of the protein assemblies and mineral particles, at least 50 measurements were performed in each case.

Tomography tilt series of mineralized samples were acquired at nominal magnifications of × 23000 to 26,000, using Tecnai 12 transmission electron microscope (FEI, Hillsboro, OR) equipped with a LaB6 filament at 120 KV. The micrographs were recorded automatically using bottom mounted Gatan 2000 CCD camera. The micrographs were taken in a tilt range from −60° to +60° with of 1° increment from −45° to 45° and 0.5° increment from −60° to −45°and from 45° to 60°. Because of the strong contrast of mineralized samples, the images were aligned using fiducial-less procedure in IMOD reconstruction package (University of Colorado, Boulder, CO) (56). Three-dimensional density maps were reconstructed from the tilt series images using Chimera software (University of California, San Francisco, CA (57)).

RESULTS

Self-assembly of rM179 in the Presence of Reconstituted Collagen Fibrils—The collagen assembly was carried out at 37 °C on the carbon-coated TEM grids as described elsewhere (9). The collagen fibrils were several microns long and had an average diameter of 162 ± 37 nm. Negatively stained fibrils showed a banding pattern with periodicity of ~67 nm, characteristic of collagen type I D-spacing (Fig. 1*A* and supplemental Fig. S2). After the deposition of collagen fibrils, amelogenin assembly was carried out on the same grid at a pH adjusted to 8.0–8.3. The TEM studies of negatively stained samples revealed two populations of amelogenin self-assemblies: homogeneous amelogenin assemblies and assemblies associated with collagen fibrils. Amelogenin not associated with collagen fibrils self-assembled into individual nanospheres of average diameter 17.6 ± 2.6 nm with very few larger aggregates (Fig. 1*A*), which is in an agreement with literature reports of amelogenin self-assembly at pH 8.0 and above (25, 26), and our control amelogenin self-assembly experiments without collagen fibrils (supplemental Fig. S3). At the same time, long chains of nanospheres, 12 ± 2.3 nm in diameter were observed in association with collagen fibrils. These chains were aligned with the long axis of the fibril, in many instances the individual nanospheres in the chains fused together, forming filamentous structures (Fig. 1, *B* and *C*).

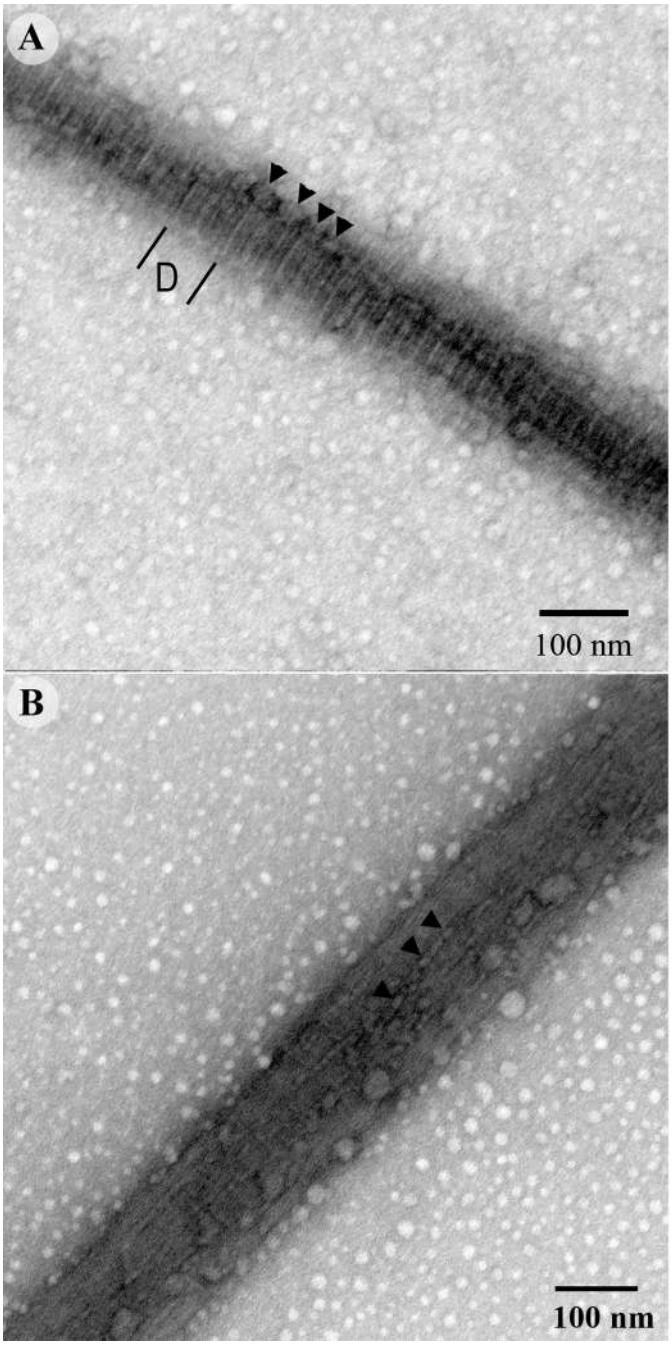

FIGURE 1. **TEM micrographs of collagen fibrils incubated with amelogenin and negatively stained, at low (*A*) and intermediate (*B*) magnifications.** Note the chains of nanospheres and fused filamentous amelogenin assemblies associated with collagen fibrils, indicated by *arrowheads*.

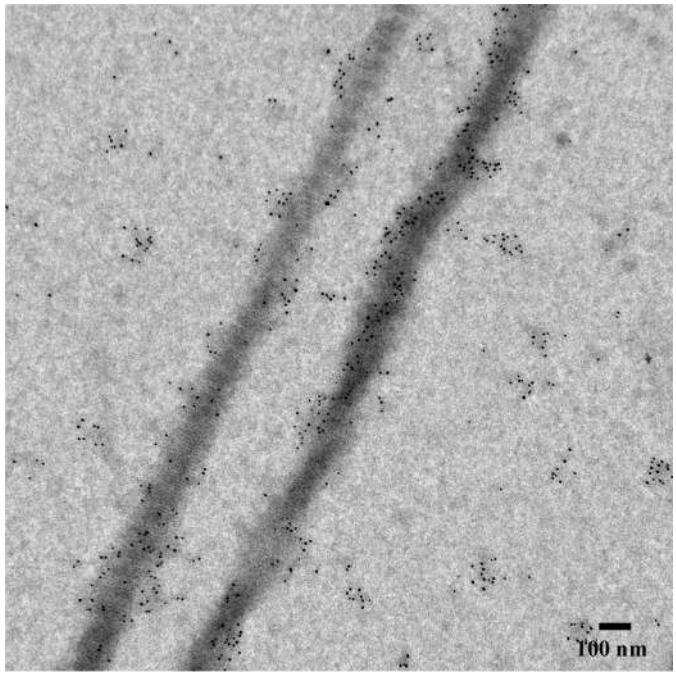

FIGURE 2. **TEM micrographs of collagen fibrils incubated with amelogenin and labeled with amelogenin antibodies.**

We have also performed immunogold labeling of the samples using murine amelogenin antibodies, to further confirm that amelogenin binds to collagen fibrils (Fig. 2). The average density of the gold particles on the grid was 397.2 (S.D. = 94.84) p/μm^2, while on the carbon grid it was 67.8 (S.D. = 33.75) p/μm^2. The difference was significant ($p = 0.0007$) suggesting that amelogenin preferably binds to collagen fibrils. In the control samples containing collagen fibrils without amelogenin there were very few gold particles, which were randomly distributed throughout the grid (supplemental Fig. S4*A*), indicating that the observed preferential binding was not due to the cross-reactivity of amelogenin antibodies with collagen fibrils. As an additional control, we performed immunolabeling with amelogenin assembled on the grid. In this case, a high density of randomly distributed gold particles was observed (supplemental Fig. S4*B*).

Mineralization of Collagen Fibrils in the Presence of rM179—When collagen fibrils were exposed to the mineralization solution without amelogenin, typical plate-like mineral crystals randomly distributed on the grid were observed. The reconstituted collagen fibrils alone did not have any effect on the distribution or organization of the mineral (supplemental Fig. S5).

Calcium phosphate mineralization in the presence of rM179 (0.5 mg/ml) and reconstituted collagen fibrils was studied as a function of incubation time. The samples were analyzed after 2, 3, 4, and 16 h from the beginning of the reaction. Progression of the mineralization was monitored by measuring changes in the pH, as reported elsewhere (27), while the changes in mineral phase, morphology, and organization were studied using TEM, electron tomography, and electron diffraction (SAED).

After 2 h, the pH of the mineralizing solution dropped to pH 7.6 from the initial pH of 8.2. TEM analyses of the samples revealed small randomly shaped mineral particles, 8.1 $\pm$ 1.4 nm across (Fig. 3, *A* and *B*) that were distributed evenly throughout the grid. The small particles formed larger aggregates, 54 $\pm$ 14 nm across, which were mostly associated with the collagen fibrils. SAED analysis of the sample indicated the presence of an amorphous mineral phase, characterized by the diffused ring diffraction pattern (Fig. 3*A*, *inset*). In addition to these large mineral aggregates, a few filamentous mineral structures, 3–4 nm across were also observed. These A close examination of these filaments at high magnification suggest that they are chains of smaller particles (Fig. 3*C*). A detailed analysis of TEM images revealed low electron density rings around mineral par-

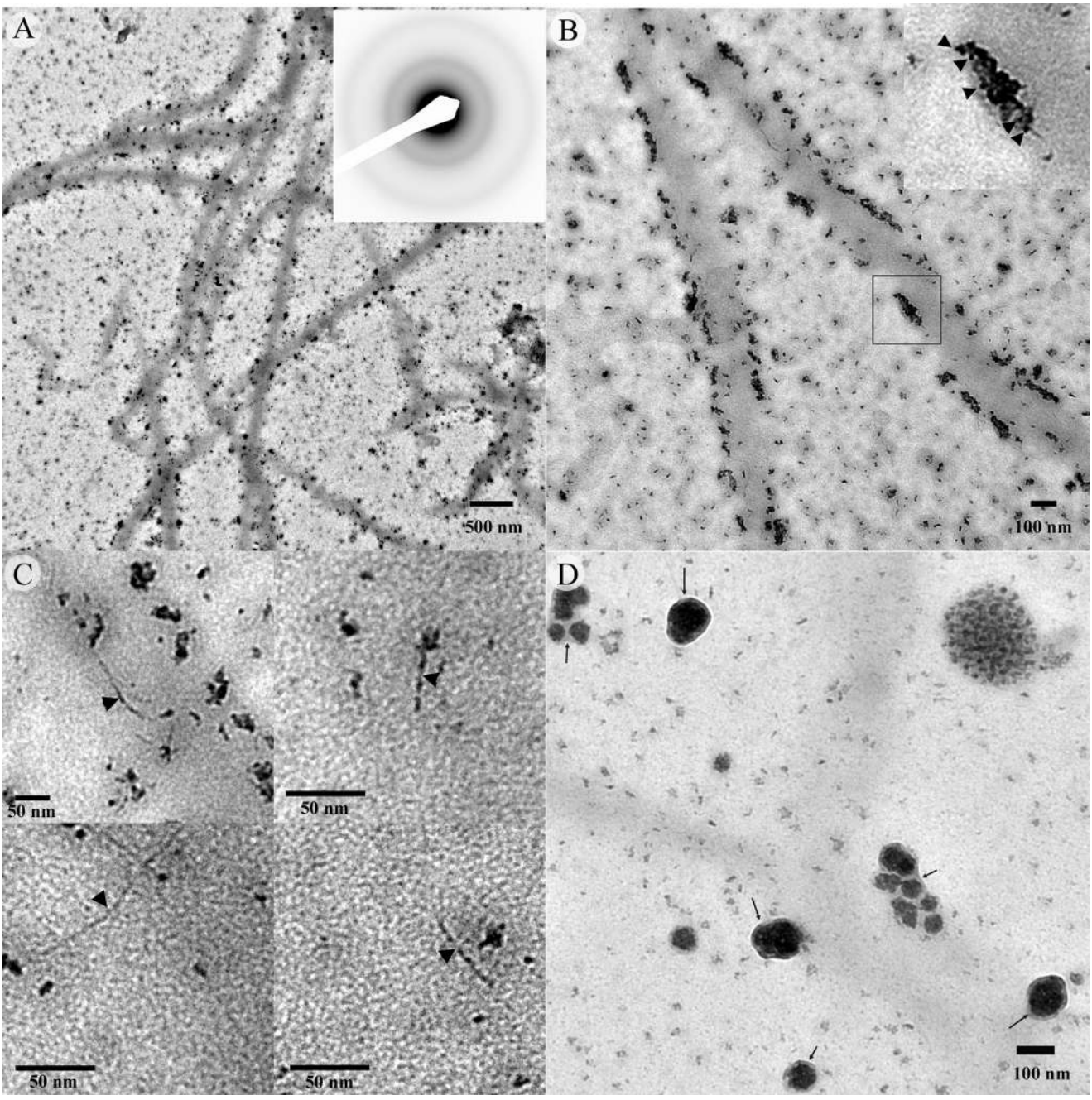

FIGURE 3. **TEM micrographs of unstained collagen fibrils mineralized in the presence of amelogenin for 2 h, at low (*A*) and intermediate (*B*) magnifications.** The diffraction pattern in the *inset* in *panel A* suggests the presence of ACP. In *panel B* a close up of the outlined mineral aggregate in the *inset*, *arrowheads* point toward individual mineral particles forming the mineral aggregate. *Panel C* shows four representative high magnification images of filamentous mineral particles (*arrowheads*). Micrograph in *D* shows the mineral particles surrounded by low electron density protein envelopes (*arrows*).

ticles and aggregates (Fig. 3*D*), which we interpret as amelogenin assemblies, suggesting co-operative interactions between amelogenin and evolving mineral phases, as has been previously proposed (27, 28).

Three hours after the beginning of the reaction, small mineral particles and larger aggregates, similar to those observed after 2 h, were still seen. At the same time, in this sample we also observed a new type of mineral particles. These were filamentous particles, 4.1 $\pm$ 0.6 nm thick and 59 $\pm$ 13 nm long, which represented a significant fraction of mineral particles in this sample. They were often associated with the large mineral aggregates (Fig. 4). Some of these particles were associated with collagen fibrils. Importantly, particles associated with the collagen fibril were organized into bundles that were co-aligned with the long axes of the fibrils (Fig. 4). SAED analysis of the mineral including the bundles of mineral filaments revealed only an amorphous mineral phase (Fig. 4*C*, *inset*). A few filamentous mineral particles were also seen in the 2-hour samples (Fig. 3*B*); however, no organized assemblies of these particles could be detected.

Four hours after the beginning of the reaction, the solution pH dropped to pH 7.4. The TEM analysis revealed ribbon-like

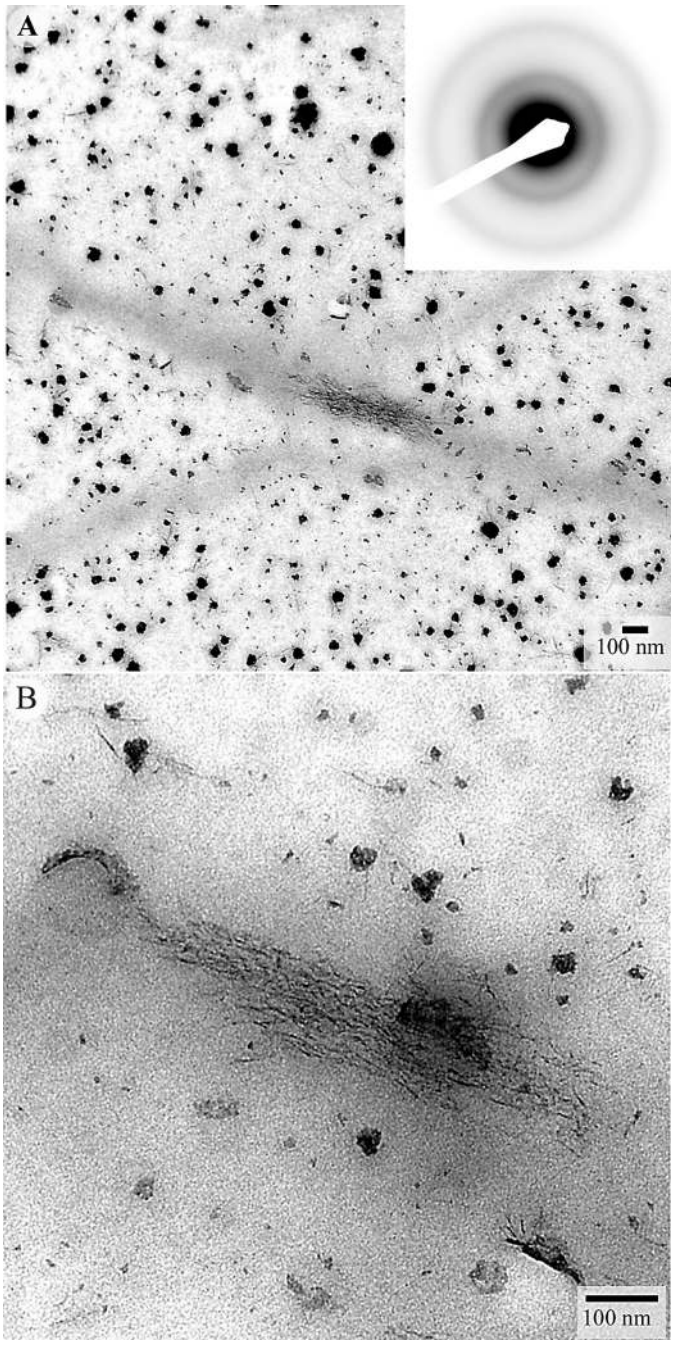

FIGURE 4. **TEM micrographs of unstained collagen fibrils mineralized in the presence of amelogenin for 3 h, at low (*A*) and high magnifications (*B*).** The diffraction pattern in the inset suggests the presence of ACP. Note the bundles of filamentous mineral on the collagen fibrils surfaces aligned with the fibril axes. Note also that elongated mineral particles similar to those forming on the collagen fibrils are distributed throughout the field of view, however, they are not organized.

particles, 60 ± 12 nm long and 2.7 ± 0.3 nm thick that were assembled into bundles with near parallel arrangement of the particles. (Fig. 5*A*). The SAED analysis indicates that these particles are comprised of poorly crystalline apatite. These data are in a good agreement with recent reports of mineralization in the presence of amelogenins (27, 28).

Beside these bundles, which were found throughout the grid, some of the mineral particles were associated with the collagen fibrils (Fig. 5, *A*–*C*). Again, particles associated with the collagen fibrils were much better organized than isolated mineral bundles described above. They were arranged in parallel arrays, co-aligned with the long fibril axis. These mineralized areas were 100–200 nm across and more than a micron long and followed all twists and turns of the associated collagen fibril, suggesting that the collagen fibrils guide the mineral deposition.

A diffraction pattern (Fig. 5*C*, *inset*) taken from the mineral aggregate associated with a collagen fibril reveals the arc-shaped reflection, corresponding to 002 plane of apatite, indicating that the mineral crystals are arranged with their crystallographic c-axes parallel to the long axis of collagen fibril. The absence of higher order reflections and low intensity of 002 reflections compared with 16-h samples (Fig. 6) also suggests that after 4 h of incubation the mineral crystals are not fully matured.

After incubation for 16 h the pH dropped to pH 6.7. TEM of the reaction products revealed higher degree of mineralization and organization of the mineral particles associated with collagen fibrils compared with the 4-h samples (Fig. 6). The mineral crystals associated with collagen fibrils were much better aligned with the collagen fibril axes than in the 4-h samples. The mineral particles had similar ribbon-like appearance; however the length (82 ± 16 nm) and thickness (3.2 ± 0.4 nm) increased indicating a progressive growth of the mineral particles. The diffraction pattern, as in the 4-h old samples, corresponded to crystalline apatite, however the number of reflections and their intensity were much higher suggesting an increase in crystallinity of the mineral (Fig. 6*A*, *inset*). Crystalline bundles not associated with collagen fibrils were also observed (Fig. 6*B*). These bundles were similar in size and organization to ones found in mineralization experiments in the presence of amelogenin alone (27, 28).

To better understand the nature of the collagen-mineral complexes, we have performed an electron tomography study of several mineralized fibrils, which were incubated for 16 h. One tomography series was carried out on a collagen fibril with low mineral content, likely representing an early stage of mineralization (Fig. 7). Two movies, a tilt series of the region shown in Fig. 7*A* and a reconstruction of the fragment shown in Fig. 7*D* are presented in Movies 1 and 2, respectively. Although mineral bundles associated with the fibril were co-aligned with the fibril axis, they were poorly organized and were surrounded by a shell of low electron density material, which we interpreted as a proteinaceous envelope surrounding the forming crystals. Similar structures were previously observed in mineralization experiments in the presence of amelogenins (27, 28). The tomographic reconstruction revealed that these aggregates were bound to the surface of the collagen fibrils and no mineral at this stage was found inside the fibrils.

Another tomography series was carried out on a highly mineralized fibril (Fig. 8). To better visualize the organization of the crystals in the mineralized fibrils, the high resolution reconstruction was performed on a 50-nm thick section of the fibril oriented in the grid plane and cutting through the middle of the fibril. The tomographic reconstruction has revealed that the mineral particles are present throughout the fibril thickness and the mineral density was higher inside the fibrils than on the

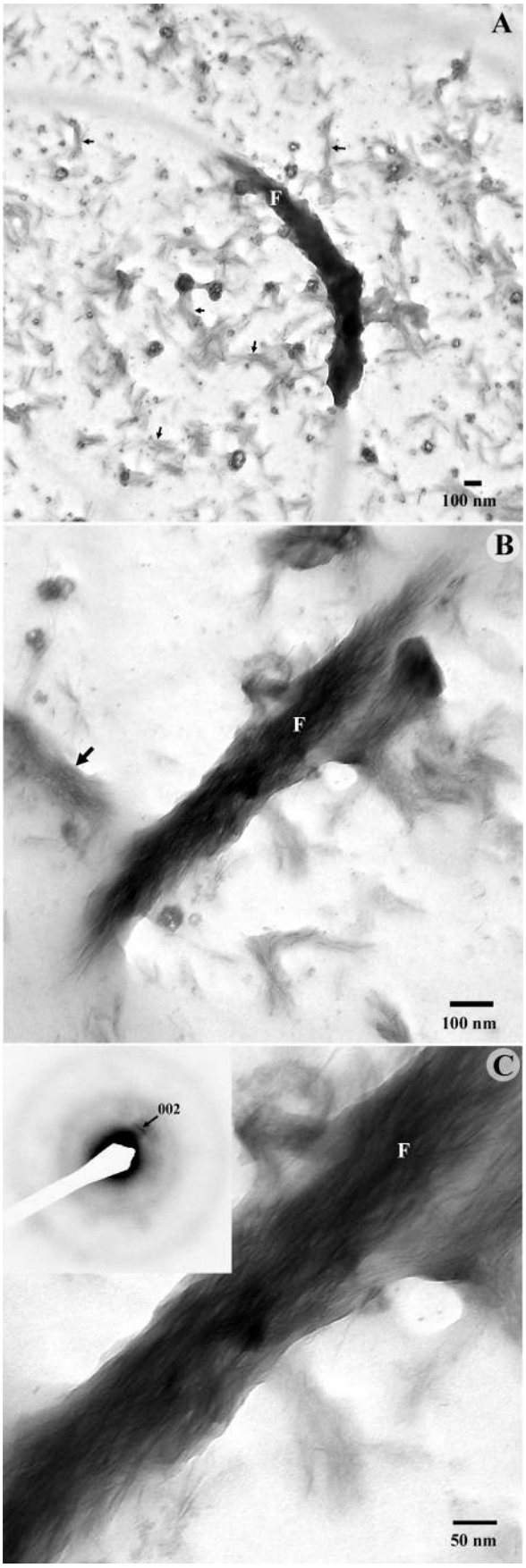

outside (Fig. 8). Two movies, a tilt series of the area shown in Fig. 8*A* and a reconstruction of the fragment shown in the bottom panel of Fig. 8 are presented in Movies 3 and 4, respectively. Interestingly, the mineral particles on the outside were larger and less organized than those inside the fibril, suggesting that collagen molecules might play a role in the organization of mineral particles inside the fibril.

The results of the tomography studies support the notion that the mineralization of the collagen fibrils in the presence of amelogenin starts on the outside of the fibrils and is guided by oriented amelogenin assemblies. Once the mineral crystals form on the surface of the fibrils the mineralization of the bulk of the fibril takes place.

DISCUSSION

We have conducted a series of experiments with the goal to determine how supramolecular complexes of collagen and amelogenin influence calcium phosphate mineral formation and structural organization. Specifically, we show that collagen fibrils can interact with amelogenin nanospheres and guide their assembly into chains and filamentous structures aligned along the fibril axis. Furthermore, the results of our study indicate that the interactions between collagen fibrils and amelogenin can regulate calcium phosphate mineralization, leading to formation of organized mineral crystal arrays associated with collagen fibrils, with their c-axes aligned with the long axis of the fibril.

The results of our protein assembly experiments show that amelogenin nanospheres interact with reconstituted collagen fibrils leading to the formation of chain-like or filamentous assemblies of amelogenin on the collagen fibril surface, aligned with the fibril axis. Amelogenin nanospheres in these higher-order assemblies were significantly smaller than the isolated nanospheres not associated with the fibrils, suggesting changes in packing of amelogenin molecules during the formation of these chains. Similar higher order assemblies of amelogenin nanospheres have been described in a number of recent studies (26, 28, 58) at pH 7.5 and below, or in the presence of Ca^{2+} ions, while at pH 8.0–8.3, maintained in our experiments, mainly isolated nanospheres were reported. The fact that in our experiments such structures were found only in association with collagen fibrils and were oriented along the fibril axes indicates that specific interactions between amelogenin and collagen fibril surfaces regulate the formation of these elongated amelogenin assemblies. In an earlier study Wiedemann-Bidlack *et al.* (26) similarly found that the diameter of isolated rM179 nanospheres (10 ± 2.5 nm) significantly decreases (7 ± 1.3 nm) upon assembly into chain-like structures at pH 7.2.

Our immunolabeling experiments further confirm the preferential binding of amelogenin to collagen fibrils. Interestingly, amelogenin has been previously reported to lack any specific

FIGURE 5. **TEM micrographs of unstained collagen fibrils mineralized in the presence of amelogenin for 4 h at low (*A*) and intermediate (*B*); *C* is a higher magnification of the fibril in *B*.** The mineral is poorly crystalline apatitic phase, based on the electron diffraction in the *inset*, which is taken from the mineralize collagen fibril (*f*) shown in *C*. Note that the 002 reflections are co-aligned with the collagen fibril axis. Also note small bundles of elongated crystals throughout the grid (*arrows*).

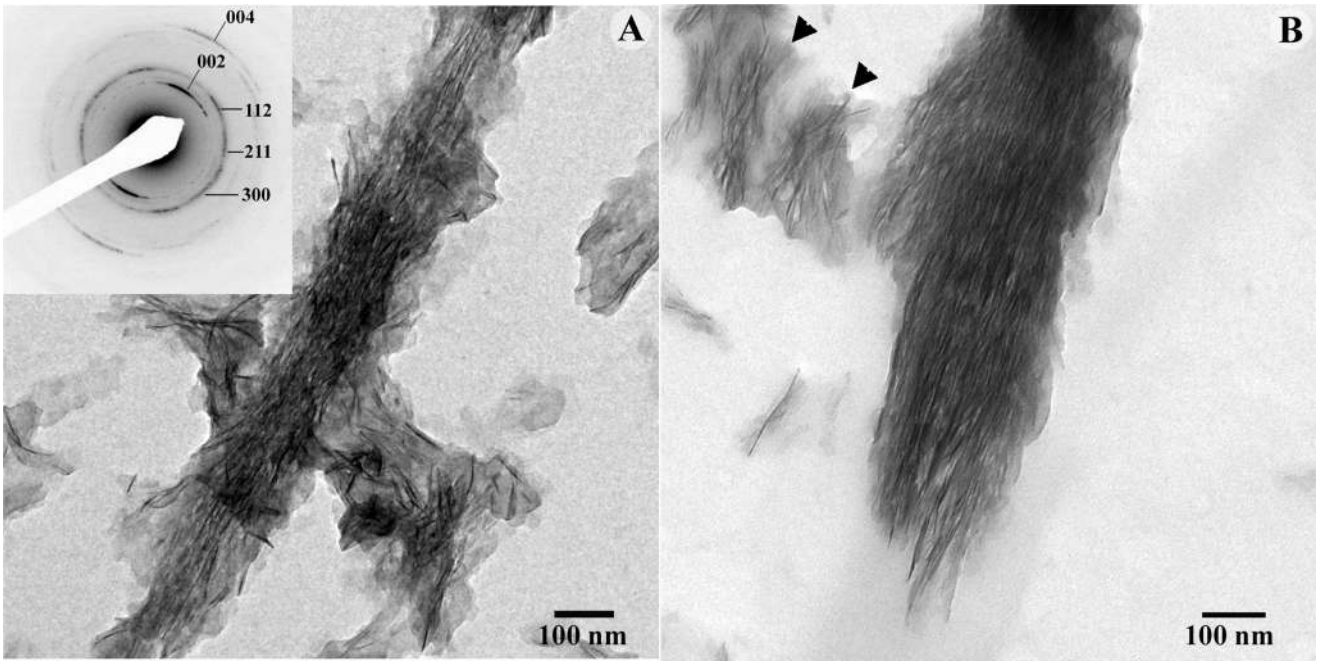

FIGURE 6. **TEM micrographs of unstained collagen fibrils mineralized in the presence of amelogenin for 16 h.** Electron diffraction pattern in the inset taken from the fibril in *A*, indicates the presence of mature apatitic crystals co-aligned with the fibril axis. Besides the mineral particles associated with collagen fibrils, bundles of elongated crystals (*arrowheads*) were observed throughout the grid (*B*).

binding affinity to gelatin (59). This discrepancy can be due to the differences in the molecular structure of denatured triple helices of gelatin *versus* the highly organized arrangement of collagen triple-helices in the fibrils (60). It is plausible that amelogenin can recognize the surfaces of collagen fibrils, with periodic molecular structure, but will not bind to denatured triple helices of gelatin. Such differences in interactions of native collagen and gelatin with other proteins have been previously reported. For example, native collagen is a much better substrate for collagenases than gelatin, because of their structural differences (61). Differences have been also reported in the binding affinity of integrins to collagen and gelatin (62, 63) Many non-collagenous proteins bind to specific regions of collagen molecules, leading to their preferred localization to particular bands of the periodic collagen fibril pattern (15–17, 64). The analysis of the amelogenin immunolabeling data has not revealed any periodicity in the gold particle distribution on the collagen fibrils, as it has been observed for other proteins, which might indicate that the nature of collagen-amelogenin interactions do not involve any localized recognition domains along the collagen molecules. Yet, the fact that the amelogenin supramolecular assemblies co-align with the fibril axis suggest a some level of specificity of these interactions which might be based on the recognition of the general structural properties of the triple helices, and their staggered arrays or, might involve weak interactions, such as hydrogen bonds between PPII regions of amelogenin and collagen.

Over the years, a number of studies have demonstrated that fibrillar type I collagen itself does not affect calcium phosphate mineralization and other factors, such as noncollagenous acidic proteins are needed to regulate this process (9–11). Here we demonstrate that the presence of amelogenin assemblies can affect the mineralization process and lead to the formation of highly organized mineral crystallite arrangements inside and outside collagen fibrils, structurally similar to the mineralized collagen fibrils of bone and dentin.

The results of our mineralization experiments indicate that the first mineral phase formed was amorphous calcium phosphate. It has to be mentioned however that at the nanoscale it might be difficult to distinguish between amorphous phases and nanocrystals which are only a few unit cells across. Nevertheless, our results are in a good agreement with recent literature reports, showing that the full-length amelogenin transiently stabilizes ACP *in vitro* (27) and that transient ACP is present in early secretory enamel *in vivo* (65).

Interestingly, alongside with randomly shaped mineral particles and aggregates, highly anisotropic needle shaped or filamentous mineral particles were observed after 3 h in the reaction. These particles were observed throughout the grid and not only in association with collagen fibrils which suggests that the shape of these elongated particles is primarily regulated by amelogenin, whose ability to control calcium phosphate mineral growth has been previously shown in a number of studies (27, 28, 55). Interestingly, the SAED analysis of 3-h samples revealed only amorphous mineral phase, implying that the elongated shape of the particles is determined before the crystallization takes place. We have recently reported that the morphology and structural organization of initial amorphous mineral particles in secretory enamel is similar to more mature crystalline mineral structures (65). Our data presented here further support the notion that enamel matrix proteins, and amelogenin, in particular, play the major role in the regulation of mineral morphology in secretory enamel.

Whereas the elongated mineral particles were randomly distributed across the grid in 3-h samples, a number of organized bundles of these particles were found on the collagen fibrils.

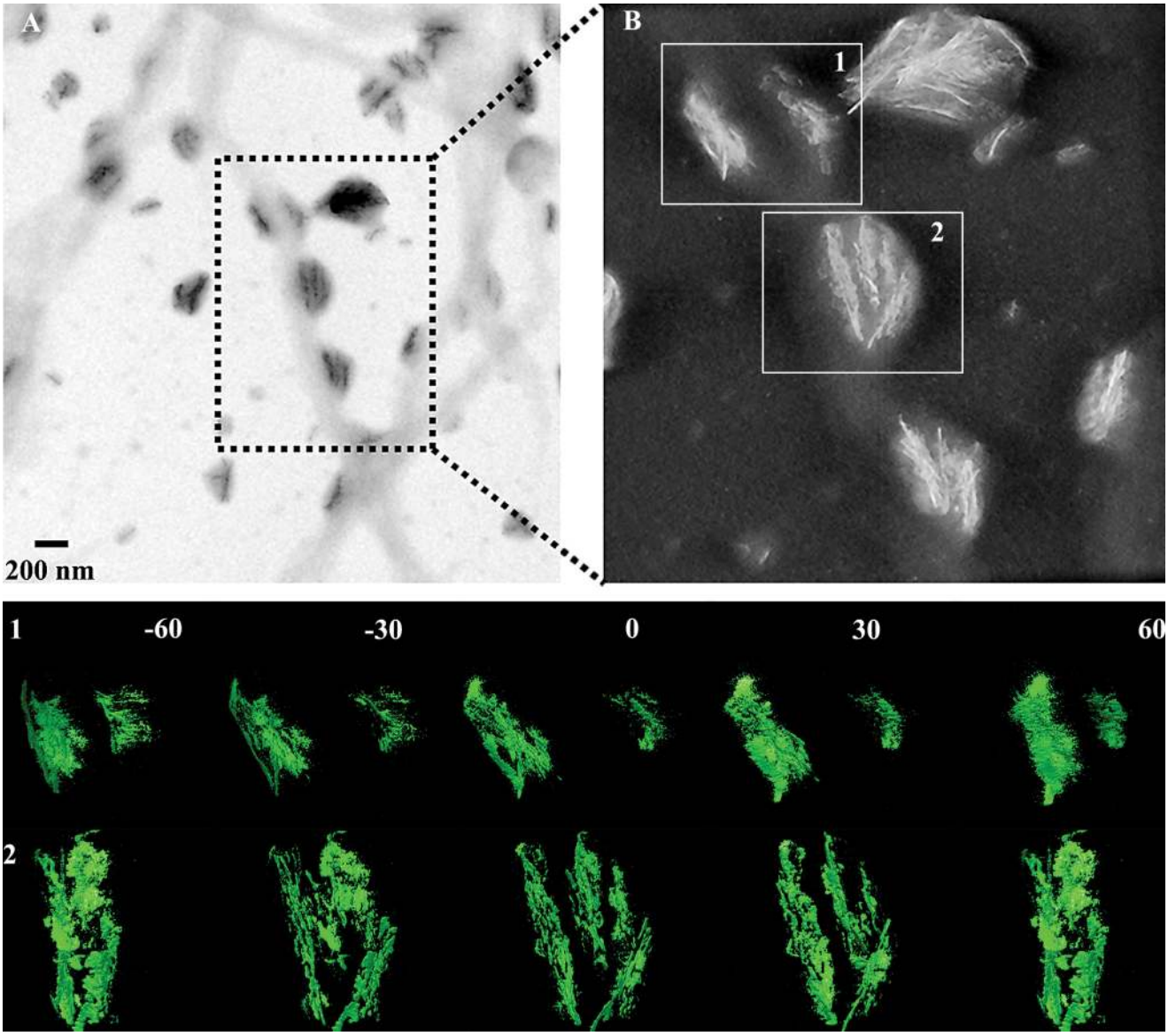

FIGURE 7. *A*, TEM micrograph of a collagen fibril with mineral bundles attached at its surface. *B*, a tomographic reconstruction of the area outlined in *A*. 1 and 2 are views from different angles at mineralized bundles indicated in *B* as *areas 1* and *2*.

Despite their amorphous nature, these bundles were similar to the bundles of apatitic crystals associated with collagen fibrils, which were observed at longer incubation times. Specifically, the long axes of the particles in these bundles were co-aligned with the fibril axes. This observation suggests that collagen fibrils influence the organization of mineral particles on their surface, possibly via interactions with amelogenin assemblies associated with the mineral. As discussed above our data strongly indicate the presence of specific interactions between collagen fibrils and amelogenin, which lead to formation of elongated amelogenin assemblies aligned with the long axes of collagen fibrils. We believe that such interactions can lead to organization of mineral particles along the fibril.

After 4 h the majority of mineral particles were apatitic nanocrystals based on the diffraction analysis. Two groups of mineral particles were observed. One group, not associated with collagen fibrils, consisted of relatively small bundles of aligned crystals, similar to the crystalline arrays reported in earlier studies of calcium phosphate mineralization in the presence of amelogenin (27, 28). Second group consisted of the large arrays of elongated mineral crystals, co-aligned with the fibril axes. These crystalline arrays were wider, longer and much better aligned than the bundles not associated with collagen. Interestingly, these mineralized bundles were often up to 2 times wider than the diameter of the collagen fibrils, with which they are associated. Our tomography data further show that these arrays originate at the surface of the collagen fibrils and at the later stages propagate into the bulk of the fibrils. The analysis of the tomographic reconstructions revealed that there are two populations of crystals in these bundles. One consists of small well-aligned crystals inside the collagen fibrils, while another is comprised of larger and less aligned crystals on the periphery of the fibrils. These observations suggest that the mineral arrays are comprised of two portions, one on the outside controlled by the amelogenin assemblies aligned on the collagen fibril and the inner portion which is guided by the

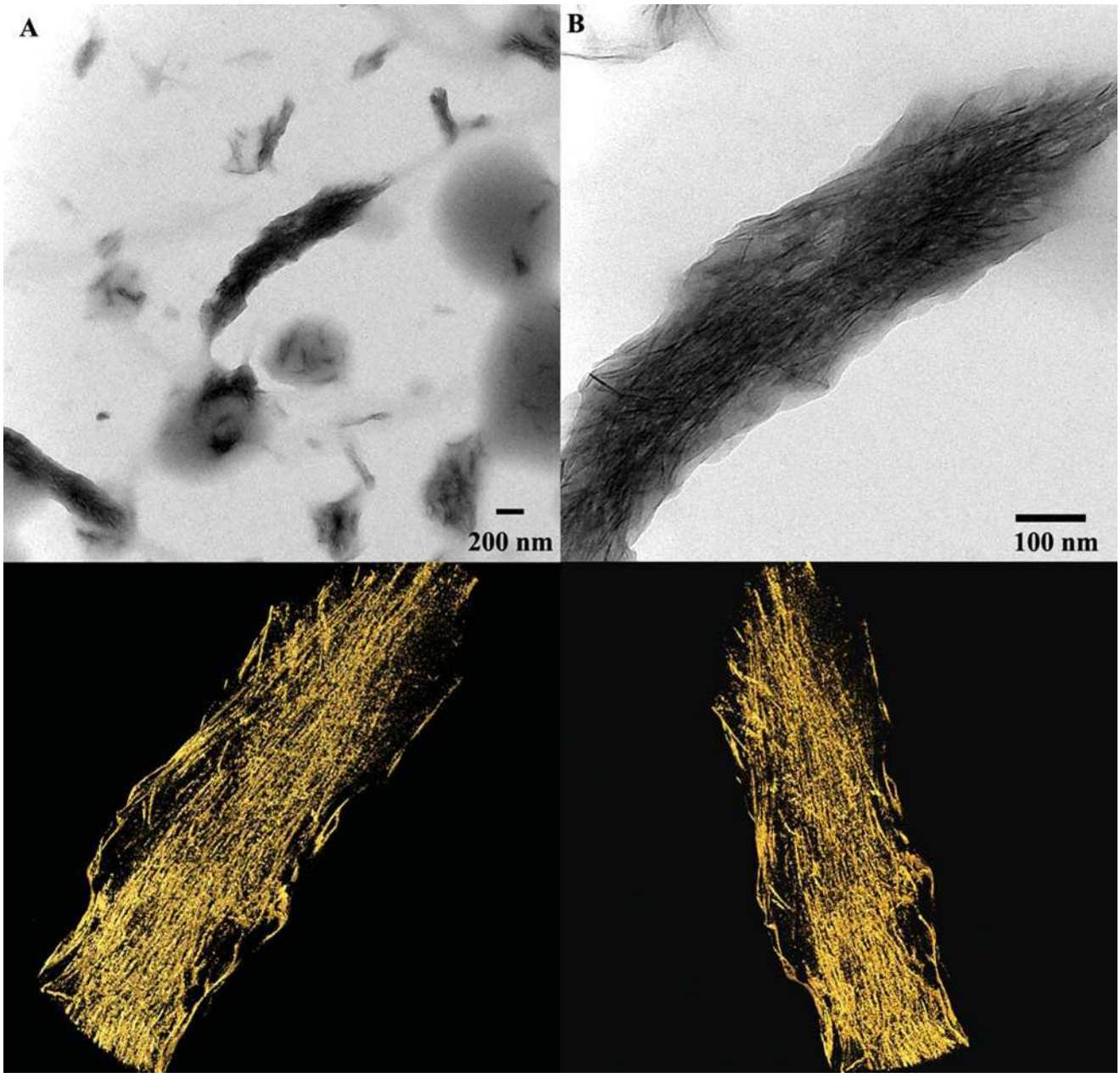

FIGURE 8. *A*, TEM micrographs of fully mineralized collagen fibril at low (*A*) and high magnifications (*B*). Three-dimensional reconstructions of the mineralized fibril from two different angles are shown in the bottom panel.

organization of triple helices in the collagen fibril. We believe that these arrays develop from the bundles of amorphous mineral particles, observed on the surface of collagen fibrils in 3-h samples.

Overall, the results of our *in vitro* study show that the amelogenin assemblies interact with forming mineral and lead to the formation of elongated amorphous particles, while the interactions between collagen fibrils and amelogenin assemblies lead to the oriented deposition of the mineral on the surface of the fibrils. After crystallization, the mineral particles induce oriented crystal nucleation and growth inside the collagen fibrils leading to the formation of continuous network of organized crystals in and around the fibril. These data support the hypothesis that amelogenin can regulate collagen fibrils mineralization at the DEB and facilitate the continuity of mineral and organic phases between dentin and enamel. At the same time, the DEB is a complex structure, containing other matrix macromolecules which might play important roles in the formation and function of this boundary. Further studies are needed to gain a better understanding of this fascinating interface.

CONCLUSION

We show that full-length amelogenin can organize into chain-like or filamentous structures on the surface of collagen fibrils. Furthermore, the interactions between collagen fibrils, amelogenin assemblies and mineral particles lead to mineralization of collagen fibrils. The mineral crystals organize on the outside and inside of collagen fibrils in parallel arrays with c-axes of the crystals co-aligned with the fibril axis, similar to the crystal organization in the native collagen fibrils. Collec-

tively, these results suggest that amelogenin might play a role in collagen mineralization at the dentino-enamel boundary and facilitate the formation of robust interactions between mineral and organic phases of dentin and enamel at the molecular level. We believe that these results provide novel insight into formation and stability of this unique interface.

Acknowledgments—We thank Dr. Peijun Zhang for her help in the analysis of the tomographic data. Electron microscopy studies were conducted at the Center for Biological Imaging, the Department of Structural Biology at the University of Pittsburgh and the Department of Materials Science and Engineering, Carnegie Mellon University, Pittsburgh. Support for electron tomography studies was provided by Dr. James Conway of the UPSOM Department of Structural Biology, including Commonwealth of Pennsylvania Grant SAP 4100031302, with assistance from Drs. Peijun Zhang and Alexander Makhov.

REFERENCES

1. Nanci, A. (2007) *Ten Cate's Oral Histology: Development, Structure, and Function*, Mosby, St. Louis, MO
2. Weiner, S., and Wagner, H. D. (1998) *Annu. Rev. Materials Sci.* **28,** 271–298
3. Landis, W. J., Hodgens, K. J., Arena, J., Song, M. J., and McEwen, B. F. (1996) *Microsc. Res. Tech.* **33,** 192–202
4. Weiner, S., and Traub, W. (1992) *FASEB J.* **6,** 879–885
5. Brodsky, B., and Ramshaw, J. A. M. (1997) *Matrix Biol.* **15,** 545–554
6. Brodsky, B., and Shah, N. K. (1995) *FASEB J.* **9,** 1537–1546
7. Chapman, J. A. (1974) *Connect. Tissue Res.* **2,** 137–150
8. Kadler, K. E., Holmes, D. F., Trotter, J. A., and Chapman, J. A. (1996) *Biochem. J.* **316,** 1–11
9. Deshpande, A. S., and Beniash, E. (2008) *Cryst. Growth Des.* **8,** 3084–3090
10. Hunter, G. K., Poitras, M. S., Underhill, T. M., Grynpas, M. D., and Goldberg, H. A. (2001) *J. Biomed. Mater. Res.* **55,** 496–502
11. Saito, T., Arsenault, A. L., Yamauchi, M., Kuboki, Y., and Crenshaw, M. A. (1997) *Bone* **21,** 305–311
12. Boskey, A. L. (1998) *J. Cell. Biochem.* 83–91
13. Hunter, G. K., and Goldberg, H. A. (1994) *Biochem. J.* **302,** 175–179
14. Hunter, G. K., Hauschka, P. V., Poole, A. R., Rosenberg, L. C., and Goldberg, H. A. (1996) *Biochem. J.* **317,** 59–64
15. Beniash, E., Traub, W., Veis, A., and Weiner, S. (2000) *J. Struct. Biol.* **132,** 212–225
16. Dahl, T., Sabsay, B., and Veis, A. (1998) *J. Struct. Biol.* **123,** 162–168
17. Di Lullo, G. A., Sweeney, S. M., Korkko, J., Ala-Kokko, L., and San Antonio, J. D. (2002) *J. Biol. Chem.* **277,** 4223–4231
18. He, G., and George, A. (2004) *J. Biol. Chem.* **279,** 11649–11656
19. Margolis, H. C., Beniash, E., and Fowler, C. E. (2006) *J. Dent. Res.* **85,** 775–793
20. Delak, K., Harcup, C., Lakshminarayanan, R., Sun, Z., Fan, Y., Moradian-Oldak, J., and Evans, J. S. (2009) *Biochemistry* **48,** 2272–2281
21. Goto, Y., Kogure, E., Takagi, T., Aimoto, S., and Aoba, T. (1993) *J. Biochem.* **113,** 55–60
22. Lakshminarayanan, R., Fan, D., Du, C., and Moradian-Oldak, J. (2007) *Biophys. J.* **93,** 3664–3674
23. Lakshminarayanan, R., Yoon, I., Hegde, B. G., Fan, D., Du, C., and Moradian-Oldak, J. (2009) *Proteins* **76,** 560–569
24. Matsushima, N., Izumi, Y., and Aoba, T. (1998) *J. Biochem.* **123,** 150–156
25. Moradian-Oldak, J., Paine, M. L., Lei, Y. P., Fincham, A. G., and Snead, M. L. (2000) *J. Struct. Biol.* **131,** 27–37
26. Wiedemann-Bidlack, F. B., Beniash, E., Yamakoshi, Y., Simmer, J. P., and Margolis, H. C. (2007) *J. Struct. Biol.* **160,** 57–69
27. Kwak, S. Y., Wiedemann-Bidlack, F. B., Beniash, E., Yamakoshi, Y., Simmer, J. P., Litman, A., and Margolis, H. C. (2009) *J. Biol. Chem.* **284,** 18972–18979
28. Beniash, E., Simmer, J. P., and Margolis, H. C. (2005) *J. Struct. Biol.* **149,** 182–190
29. Dong, X. D., and Ruse, N. D. (2003) *J. Biomed. Mater. Res. A.* **66,** 103–109
30. Imbeni, V., Kruzic, J. J., Marshall, G. W., Marshall, S. J., and Ritchie, R. O. (2005) *Nat. Mater.* **4,** 229–232
31. Lin, C. P., and Douglas, W. H. (1994) *J. Dent. Res.* **73,** 1072–1078
32. Marshall, G. W., Jr., Balooch, M., Gallagher, R. R., Gansky, S. A., and Marshall, S. J. (2001) *J. Biomed. Mater. Res.* **54,** 87–95
33. Xu, H. H., Smith, D. T., Jahanmir, S., Romberg, E., Kelly, J. R., Thompson, V. P., and Rekow, E. D. (1998) *J. Dent. Res.* **77,** 472–480
34. Veis, A. (2005) *Science* **307,** 1419–1420
35. Zaslansky, P., Friesem, A. A., and Weiner, S. (2006) *J. Struct. Biol.* **153,** 188–199
36. Wang, R. Z., and Weiner, S. (1998) *J. Biomech.* **31,** 135–141
37. Lester, K. S., and Boyde, A. (1967) *Calcif. Tissue Int.* **1,** 273–287
38. Arsenault, A. L., and Robinson, B. W. (1989) *Calcif. Tissue Int.* **45,** 111–121
39. Hayashi, Y. (1992) *J. Electron Microsc.* **41,** 387–391
40. Bodier-Houllé, P., Steuer, P., Meyer, J. M., Bigeard, L., and Cuisinier, F. J. G. (2000) *Cell Tissue Res.* **301,** 389–395
41. Nanci, A., Zalzal, S., Lavoie, P., Kunikata, M., Chen, W., Krebsbach, P. H., Yamada, Y., Hammarström, L., Simmer, J. P., Fincham, A. G., Snead, M. L., and Smith, C. E. (1998) *J. Histochem. Cytochem.* **46,** 911–934
42. Papagerakis, P., MacDougall, M., Hotton, D., Bailleul-Forestier, I., Oboeuf, M., and Berdal, A. (2003) *Bone* **32,** 228–240
43. Bègue-Kirn, C., Krebsbach, P. H., Bartlett, J. D., and Butler, W. T. (1998) *Eur. J. Oral Sci.* **106,** 963–970
44. Bleicher, F., Couble, M. L., Farges, J. C., Couble, P., and Magloire, H. (1999) *Matrix Biol.* **18,** 133–143
45. Beniash, E., Skobe, Z., and Bartlett, J. D. (2006) *Eur. J. Oral Sci.* **114,** 24–29
46. Papagerakis, P., Lin, H. K., Lee, K. Y., Hu, Y., Simmer, J. P., Bartlett, J. D., and Hu, J. C. C. (2008) *J. Dent. Res.* **87,** 56–59
47. Gibson, C. W., Yuan, Z. A., Hall, B., Longenecker, G., Chen, E., Thyagarajan, T., Sreenath, T., Wright, J. T., Decker, S., Piddington, R., Harrison, G., and Kulkarni, A. B. (2001) *J. Biol. Chem.* **276,** 31871–31875
48. Hart, P. S., Aldred, M. J., Crawford, P. J., Wright, N. J., Hart, T. C., and Wright, J. T. (2002) *Arch. Oral Biol.* **47,** 261–265
49. Hu, J. C., Chun, Y. H., Al Hazzazzi, T., and Simmer, J. P. (2007) *Cells Tissues Organs* **186,** 78–85
50. Kim, J. W., Nam, S. H., Jang, K. T., Lee, S. H., Kim, C. C., Hahn, S. H., Hu, J. C., and Simmer, J. P. (2004) *Hum. Genet.* **115,** 248–254
51. George, A., and Veis, A. (2008) *Chem. Rev.* **108,** 4670–4693
52. Silverman, L., and Boskey, A. L. (2004) *Calcif. Tissue Int.* **75,** 494–501
53. Miller, E. J., and Rhodes, R. K. (1982) *Methods Enzymol.* **82,** 33–64
54. Simmer, J. P., Lau, E. C., Hu, C. C., Aoba, T., Lacey, M., Nelson, D., Zeichner-David, M., Snead, M. L., Slavkin, H. C., and Fincham, A. G. (1994) *Calcif. Tissue Int.* **54,** 312–319
55. Moradian-Oldak, J., Tan, J., and Fincham, A. G. (1998) *Biopolymers* **46,** 225–238
56. Kremer, J. R., Mastronarde, D. N., and McIntosh, J. R. (1996) *J. Struct. Biol.* **116,** 71–76
57. Goddard, T. D., Huang, C. C., and Ferrin, T. E. (2007) *J. Struct. Biol.* **157,** 281–287
58. Moradian-Oldak, J., Du, C., and Falini, G. (2006) *Eur. J. Oral Sci.* **114,** 289–296
59. Hoang, A. M., Klebe, R. J., Steffensen, B., Ryu, O. H., Simmer, J. P., and Cochran, D. L. (2002) *J. Dent. Res.* **81,** 497–500
60. Veis, A., and Cohen, J. (1960) *Nature* **186,** 720–721
61. McCroskery, P. A., Wood, S., Jr., and Harris, E. D., Jr. (1973) *Science* **182,** 70–71
62. Tuckwell, D. S., Ayad, S., Grant, M. E., Takigawa, M., and Humphries, M. J. (1994) *J. Cell Sci.* **107,** 993–1005
63. Zaman, M. H. (2007) *Biophys. J.* **92,** L17–L19
64. Keene, D. R., San Antonio, J. D., Mayne, R., McQuillan, D. J., Sarris, G., Santoro, S. A., and Iozzo, R. V. (2000) *J. Biol. Chem.* **275,** 21801–21804
65. Beniash, E., Metzler, R. A., Lam, R. S., and Gilbert, P. U. (2009) *J. Struct. Biol.* **166,** 133–143